Spontaneous tubulation of membranes and vesicles reveals membrane tension generated by spontaneous curvature – Electronic Supplementary Information (ESI)

Reinhard Lipowsky [a]

This Electronic Supplementary Information (ESI) contains two appendices with some technical details of the calcuations:
App. A on 'Spontaneous curvature induced by adsorption' and App. B on 'Stress-free shapes of spherical and cylindrical membranes'.

Appendix A: Spontaneous curvature induced by adsorption

In this appendix, the membrane is viewed as an ultrathin film bounded by two surfaces or membrane/water interfaces. These two surfaces are characterized by a certain surface tension that depends on the coverage of the adsorbed 'particles', which may be atomic ions, small molecules, or macromolecules such as peptides and proteins. For simplicity, I will focus on a single species of adsorbing particles; the case with several species of such particles has been discussed in Refs. [1,2], albeit in a rather condensed manner.

A.1 Langmuir-type adsorption onto membrane surfaces.

The membrane is described as an ultrathin film of thickness ℓ_{me} that separates the aqueous medium into two compartments, an interior and an exterior one, compare Fig. 3. Let us now focus, for the time being, on one of these compartments, and denote the corresponding molar concentration by C. The membrane surface exposed to this compartment provides a certain number of binding sites for the adsorbing particles. The surface density of these binding sites is denoted by $1/A_{\mathrm{bs}}$, i.e., the average separation of binding sites is equal to $\sqrt{A_{\mathrm{bs}}}$.

When one particle is adsorbed onto the membrane surface, it will cover a certain surface area denoted by A_{pa}. As shown in Fig. 3 and

[a] *Theory and Bio-Systems, Max Planck Institute of Colloids and Interfaces, 14424 Potsdam, Germany; Fax: +49 331 567 9602; Tel: +49 331 567 9600; E-mail: lipowsky@mpikg.mpg.de*

Fig. 8, it is assumed here that the particle size is small compared to the membrane thickness $l_{me} \simeq 4\,\text{nm}$, i.e., that the area A_{pa} is small compared to $l_{me}^2 \simeq 16\,\text{nm}^2$.

For a membrane surface of area A, the maximal number N_{max} of particles that can be adsorbed onto this surface depends on the relative size of A_{pa} and A_{bs} according to

$$
\begin{aligned}
N_{max} &= A/A_{pa} \quad &\text{for} \quad A_{pa} > A_{bs} \\
&= A/A_{bs} \quad &\text{for} \quad A_{bs} > A_{pa} .
\end{aligned}
\tag{A.1}
$$

The maximal coverage

$$
\Gamma_{max} \equiv N_{max}/A
\tag{A.2}
$$

of the membrane surface is then given by

$$
\begin{aligned}
\Gamma_{max} &= 1/A_{pa} \quad &\text{for} \quad A_{pa} > A_{bs} \\
&= 1/A_{bs} \quad &\text{for} \quad A_{bs} > A_{pa} .
\end{aligned}
\tag{A.3}
$$

In general, the maximal coverage can vary over a wide range. If both areas A_{bs} and and A_{pa} are comparable to the area of a lipid head group, the maximal coverage Γ_{max} will be of the order of $1/\text{nm}^2$. On the other hand, if the binding sites are provided by membrane-anchored molecules that represent a minority component in the membrane and cover only 1 percent of the membrane area, the maximal coverage Γ_{max} will be of the order of $1/(100\,\text{nm}^2)$.

For each binding site, the adsorption rate is proportional to the concentration C and, thus, has the form $\kappa_{on} C$ while desorption is an activated process with rate ω_{off}. The number N of particles adsorbed onto the membrane surface under consideration then changes with time t according to

$$
dN/dt = \kappa_{on} C (N_{max} - N) - \omega_{off} N .
\tag{A.4}
$$

If the adsorbing particles are added at time $t = t_0$, the number N increases with time according to

$$
N(t) = N_{max} \frac{C}{K_d + C} \left[1 - e^{-\omega(t-t_0)} \right]
\tag{A.5}
$$

with the equilibrium constant

$$
K_d \equiv \omega_{off}/\kappa_{on}
\tag{A.6}
$$

and the relaxation rate

$$
\omega = \kappa_{on} C + \omega_{off} .
\tag{A.7}
$$

Chemical equilibrium between the membrane surface and the bulk is reached in the long-time limit, which implies the equilibrium value

$$N(\infty) = N_{\mathrm{max}} \frac{C}{K_{\mathrm{d}} + C}. \tag{A.8}$$

The corresponding value of the surface coverage Γ is then given by

$$\Gamma \equiv \frac{N(\infty)}{A} = \Gamma_{\mathrm{max}} \frac{C}{K_{\mathrm{d}} + C} \tag{A.9}$$

which implies

$$\Gamma \approx \Gamma_{\mathrm{max}} \frac{C}{K_{\mathrm{d}}} \quad \text{for} \quad C \ll K_{\mathrm{d}} \tag{A.10}$$

and

$$\Gamma \approx \Gamma_{\mathrm{max}} \quad \text{for} \quad C \gg K_{\mathrm{d}}. \tag{A.11}$$

For $C = K_{\mathrm{d}}$, the expressions (A.10) and (A.11) differ from (A.9) only by a factor $\frac{1}{2}$ and, thus, still provide order of magnitude estimates for Γ.

A.2 Concentration dependence of surface tensions.

For a planar surface, the equilibrium coverage Γ_{eq} is related to the surface tension Σ via the Gibbs adsorption equation as given by

$$\Gamma = -(\partial \Sigma / \partial \mu)_T \tag{A.12}$$

where μ is the chemical potential of the adsorbing particle species. For dilute solutions, the chemical potential has the form $\mu = \mu_0 + k_{\mathrm{B}} T \ln(C/C_0)$ which implies

$$(\partial \Sigma / \partial C)_T = -k_{\mathrm{B}} T \Gamma / C. \tag{A.13}$$

Inserting the expression (A.9) for $\Gamma = \Gamma(C)$ into this latter relation, one obtains the concentration-dependent surface tension

$$\Sigma(C) = \Sigma(0) - k_{\mathrm{B}} T \Gamma_{\mathrm{max}} \ln(1 + C/K_{\mathrm{d}}) \tag{A.14}$$

for dilute solutions of the absorbing particles.

For small concentrations $C \lesssim K_{\mathrm{d}}$, this expression becomes

$$\Sigma(C) \approx \Sigma(0) - k_{\mathrm{B}} T \Gamma_{\mathrm{max}} C / K_{\mathrm{d}} \approx \Sigma(0) - k_{\mathrm{B}} T \Gamma. \tag{A.15}$$

The concentration dependence of the surface tension as given by (A.14) can now be applied to both membrane surfaces separately.

Thus, the exterior membrane surface, which is exposed to the bulk concentration C_{ex} in the exterior compartment, has the tension

$$\Sigma_{ex} \equiv \Sigma(C_{ex}) \approx \Sigma(0) - k_B T \Gamma_{ex} \tag{A.16}$$

with

$$\Gamma_{ex} \approx \Gamma_{max} \frac{C_{ex}}{K_d} \quad \text{for} \quad C_{ex} \lesssim K_d. \tag{A.17}$$

Likewise, the interior membrane surface, which is exposed to the bulk concentration C_{in} in the interior compartment, has the tension

$$\Sigma_{in} \equiv \Sigma(C_{in}) \approx \Sigma(0) - k_B T \Gamma_{in} \tag{A.18}$$

with

$$\Gamma_{in} \approx \Gamma_{max} \frac{C_{in}}{K_d} \quad \text{for} \quad C_{in} \lesssim K_d. \tag{A.19}$$

A.3 Available adsorption areas of curved membrane surfaces.

So far, a planar membrane segment as in Fig. 8(a) has been discussed. This membrane segment is now slightly curved in such a way that its volume is conserved up to first order in the curvature radii. The segment then contains a neutral surface that does not change its area.

In the absence of adsorbed particles, the bilayer membrane has constant thickness and the neutral surface corresponds to the midplane of the planar bilayer. In the presence of adsorbed particles, the bilayer thickness varies and the neutral surface is somewhat shifted from the midplane if the exterior coverage Γ_{ex} differs from the interior coverage Γ_{in}.

In general, the location of the neutral surface is obtained as follows. The bilayer consists of two leaflets or monolayers. The local thickness of one leaflet is equal to ℓ in the absence of an adsorbed particle and $\ell + h_{pa}$ in the presence of an adsorbed particle, where h_{pa} denotes the size of the particle perpendicular to the membrane. The exterior leaflet of the bilayer has the average thickness

$$\ell_{ex} = (1 - \Gamma_{ex})\ell + \Gamma_{ex}(\ell + h_{pa}). \tag{A.20}$$

whereas the interior leaflet has the average thickness

$$\ell_{in} = (1 - \Gamma_{in})\ell + \Gamma_{in}(\ell + h_{pa}). \tag{A.21}$$

Furthermore, the average thickness of the bilayer membrane is

$$\ell_{me} = \ell_{ex} + \ell_{in}. \tag{A.22}$$

This bilayer is now symmetrically partitioned into two fictitious layers of equal thickness

$$L \equiv \tfrac{1}{2}\ell_{me} = \tfrac{1}{2}(\ell_{ex} + \ell_{in}). \qquad (A.23)$$

The neutral surface corresponds to the midplane between these fictitious layers and is displaced by $\frac{1}{2}(\ell_{ex} - \ell_{in})$ from its position in the absence of adsorbed particles. This displacement is positive and negative for $\Gamma_{ex} > \Gamma_{in}$ and $\Gamma_{ex} < \Gamma_{in}$, and the neutral surface is shifted towards the exterior and interior membrane surface, respectively.

When the neutral surface is bent and aquires the mean curvature $M > 0$ as in Fig. 8(b), the area of the exterior membrane surface is increased and becomes

$$A'_{ex} \approx A(1 + 2LM) = A(1 + \ell_{me}M) \qquad (A.24)$$

to leading order in M while the area of the interior membrane surface is reduced according to

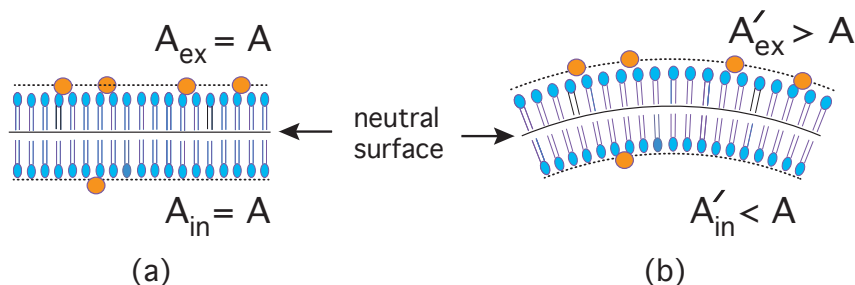$$A'_{in} \approx A(1 - 2LM) = A(1 - \ell_{me}M). \qquad (A.25)$$

Fig. 8 Available adsorption areas for (a) a planar membrane and (b) a curved membrane. In (a), the available adsorption areas A_{ex} and A_{in} of the exterior and interior membrane surface are both equal to the area A of the neutral surface. In (b), the neutral surface has again the area A but the interior and exterior surface areas are now smaller and larger than A, respectively. The two dotted lines through the particles both have the distance $L = \ell_{me}/2$ from the neural surface. Note that the neutral surface has been slightly shifted upwards because the exterior surface contains more adsorbed particles.

A.4 Free energy changes and spontaneous curvature.

The planar state in Fig. 8(a) then has the surface free energy $F_a = \Sigma_{ex}A + \Sigma_{in}A$ whereas the curved state in Fig. 8(b) has the surface free energy $F_b = \Sigma_{ex}A'_{ex} + \Sigma_{in}A'_{in}$ with $A'_{in} < A < A'_{ex}$. Thus, as

the membrane is deformed from the planar state in Fig. 8(a) to the curved state in Fig. 8(b), its surface free energy changes according to

$$\Delta F_s \equiv F_b - F_a = \Sigma_{\text{ex}}(A'_{\text{ex}} - A) + \Sigma_{\text{in}}(A'_{\text{in}} - A). \qquad (A.26)$$

Combining this relation with the expressions (A.24) and (A.25), the free energy change becomes

$$\Delta F_s \approx (\Sigma_{\text{ex}} - \Sigma_{\text{in}})\,\ell_{\text{me}}\,MA \qquad (A.27)$$

or

$$\Delta F_s \approx k_B T\,(\Gamma_{\text{ex}} - \Gamma_{\text{in}})\,\ell_{\text{me}}\,MA \qquad (A.28)$$

where the relations (A.16) and (A.18) have been used.

Finally, the surface free energy change is balanced against the bending energy $2\kappa M^2 A$ of the membrane segment by minimizing the total free energy change

$$\Delta F \equiv \Delta F_s + 2\kappa M^2 A. \qquad (A.29)$$

In principle, the bending rigidity κ may also change by the adsorption process but this change is of higher order in the coverages Γ_{ex} and Γ_{in} or the concentrations C_{ex} and C_{in}. The value $M = M_{\text{min}}$ that minimizes the total free energy change ΔF represents the spontaneous curvature

$$m \equiv M_{\text{min}} \approx \frac{k_B T}{4\kappa}\,\ell_{\text{me}}\,(\Gamma_{\text{ex}} - \Gamma_{\text{in}}) \approx \frac{k_B T}{\kappa}\,\frac{\ell_{\text{me}}\Gamma_{\text{max}}}{4}\,\frac{C_{\text{ex}} - C_{\text{in}}}{K_{\text{d}}}$$
$$(A.30)$$

where the expressions (A.17) and (A.19) have been used. Thus, the spontaneous curvature is proportional to the ratio $k_B T/\kappa$, to the membrane thickness ℓ_{me}, as well as to the coverage difference $\Gamma_{\text{ex}} - \Gamma_{\text{in}} \propto C_{\text{ex}} - C_{\text{in}}$. Note that $m > 0$ for $C_{\text{ex}} > C_{\text{in}}$ and $m < 0$ for $C_{\text{ex}} < C_{\text{in}}$ which implies that the membrane bends away from or bulges towards the compartment with the higher concentration of adsorbing particles.

App. B. Stress-free shapes of spherical and cylindrical membranes

In this Appendix, stress-free states of giant vesicles as shown in Fig. 5 with cylindrical tubules as in Fig. 6 will be considered.

B.1 Stress balance for spheres and spherical caps.

As a rather simple but instructive example, let us first consider an inflated vesicle, which attains a spherical shape with radius $R_{\rm sp}$ as shown in Fig. 5(a). For this shape, the general form (49) of the shape energy leads to the explicit expression

$$\mathcal{E}_{\rm sp} = -\Delta P \tfrac{4\pi}{3} R_{\rm sp}^3 + \Sigma 4\pi R_{\rm sp}^2 + 2\kappa m^2 R_{\rm sp}^2 - 16\pi\kappa m R_{\rm sp} + 8\pi\kappa. \tag{B.1}$$

This energy contains two terms proportional to the membrane area, $4\pi R_{\rm sp}^2$, which can be combined into the total membrane tension $\hat{\Sigma} \equiv \Sigma + 2\kappa m^2 = \Sigma + \sigma$ as in (50). The shape energy of the spherical vesicle now becomes

$$\mathcal{E}_{\rm sp} = -\Delta P \tfrac{4\pi}{3} R_{\rm sp}^3 + \hat{\Sigma} 4\pi R_{\rm sp}^2 - 16\pi\kappa m R_{\rm sp} + 8\pi\kappa. \tag{B.2}$$

In mechanical equilibrium, the radial stresses along the spherical membrane must balance which is described by

$$\partial\mathcal{E}_{\rm sp}/\partial R_{\rm sp} = 0 \tag{B.3}$$

or

$$\Delta P = 2\hat{\Sigma} M_{\rm sp} - 4\kappa m M_{\rm sp}^2 = 2\Sigma M_{\rm sp} + 4\kappa m^2 M_{\rm sp}(1 - M_{\rm sp}/m) \tag{B.4}$$

with the mean curvature $M_{\rm sp} = 1/R_{\rm sp}$ of the sphere which is identical to (52). A spherical vesicle that satisfies this radial stress balance condition will be regarded as 'stress-free'. *

The stress balance relation as given by (B.4) and (52) is a local relation that applies to any point of the spherical membrane. In fact, the same relation is obtained if we start from the shape energy of a spherical cap with curvature radius $R_{\rm sp}$. Thus, the stress balance relation (52) also applies, in particular, to the spherical caps depicted in Fig. 5.

B.2 Laplace-like equation for small $M_{\rm sp}/m$.

Inspection of (B.4) shows that the nonlinear term proportional to $M_{\rm sp}^2$ can be neglected if the spontaneous curvature m is large compared to the mean curvature $M_{\rm sp}$ of the spherical segment. In the latter case, the radial stress balance becomes

$$\Delta P \approx 2\hat{\Sigma} M_{\rm sp} = 2(\Sigma + \sigma)M_{\rm sp} \quad \text{for} \quad m \gg M_{\rm sp}. \tag{B.5}$$

---

* The intuitive term 'stress-free' is used here for all shapes that correspond to extrema of the shape energy (49). If such an extremum represents a minimum, the stress-free shape is stable; if it represents a saddle point or maximum, the stress-free shape is unstable.

The error introduced by the omission of the M_{sp}^2-term is of the order of M_{sp}/m. Thus, for a spherical vesicle with radius $R_{sp} \simeq 20\,\mu m$, this error is smaller than 10 percent if the spontaneous curvature is larger than $1/(2\mu m)$. Inspection of Table 1 shows that this situation applies to membranes decorated by anchored DNA molecules or adsorbed BAR domain proteins as well as to membranes exposed to PEG/dextran solutions.

B.3 Radial and axial stress balance for tubules.

The general expression (49) for the shape energy implies that the vesicles in Fig. 6(a,b) with one out- or one in-tube have the shape energies

$$\mathcal{E} = \mathcal{E}_{sp} \mp \Delta P \pi R_{cy}^2 L + \hat{\Sigma} 2\pi R_{cy} L \mp 4\pi\kappa m L + \pi\kappa L/R_{cy} \qquad (B.6)$$

which again depends on the total membrane tension $\hat{\Sigma} \equiv \Sigma + \sigma$. The minus sign (of the $\mp$-signs) corresponds to an out-tube, the plus sign to an in-tube.

In mechanical equilibrium, the stresses along the spherical and cylindrical membrane segments must balance. For the spherical vesicle, the radial stress balance is again described by the relations (B.4) and (B.5) discussed in the previous section. For the cylindrical tubes, the balance of radial stresses implies

$$\partial \mathcal{E}/\partial R_{cy} = 0 \quad \text{or} \quad \Delta P = 2\hat{\Sigma} M_{cy} - 4\kappa M_{cy}^3, \qquad (B.7)$$

where the latter relation holds both for out- and for in-tubes, respectively.

The retraction force at the end of the tube is given by $\partial \mathcal{E}/\partial L$, where $\partial \mathcal{E}/\partial L > 0$ leads to a shortening of the tube. It is now useful to consider an external force f which is defined in such a way that $f > 0$ corresponds to a pulling force for both out-tubes and in-tubes. The axial force balance at the tube end then has the form

$$f = \partial \mathcal{E}/\partial L \quad \text{or} \quad \pm f = \pi R_{cy}^2 \left(-\Delta P + 4\hat{\Sigma} M_{cy} - 16\kappa m M_{cy}^2 + 8\kappa M_{cy}^3 \right) \qquad (B.8)$$

where the plus and minus sign in front of f corresponds to out- and in-tubes.

The two relations (B.7) and (B.8) for the radial and axial force balance at the tube membrane can be solved for the total tension $\hat{\Sigma}$ and the pressure difference ΔP which leads to

$$\hat{\Sigma} = 8\kappa m M_{cy} - 6\kappa M_{cy}^2 \pm \tfrac{2}{\pi} f M_{cy} \qquad (B.9)$$

or

$$\Sigma = \hat{\Sigma} - \sigma = -6\kappa(M_{\text{cy}} - m)(M_{\text{cy}} - \tfrac{1}{3}m) \pm \tfrac{2}{\pi} f M_{\text{cy}} \qquad (B.10)$$

and

$$\Delta P = 16\kappa M_{\text{cy}}^2(m - M_{\text{cy}}) \pm \tfrac{4}{\pi} f M_{\text{cy}}^2, \qquad (B.11)$$

where the plus and minus signs in front of the f-terms correspond again to out- and in-tubes. Note that the substitution $M_{\text{cy}} \to -M_{\text{cy}}$, $m \to -m$, and $\Delta P \to -\Delta P$ transforms the stress balance relations (B.9) and (B.11) for the in-tube into those for the out-tube and vice versa. Since these relations are equivalent to the equations $\partial \mathcal{E}/\partial R_{\text{cy}} = 0$ and $f = \partial \mathcal{E}/\partial L$, a tube that satisfies these two relations with $f = 0$ will be considered as stress-free.

B.4 Mechanical balance between spherical caps and cylindrical tubules.

So far, the spherical vesicle and the cylindrical tubes have been considered separately. Now, I take into account that these two segments belong to the same membrane, which implies that the stress balance relations (B.9) and (B.11) for the tube must be fulfilled together with the stress balance relation (B.4) for the spherical membrane segment.[3]

A combination of the three equations (B.4), (B.9), and (B.11) eliminates both the pressure difference ΔP and the tension $\hat{\Sigma}$ and leads to the cubic equation

$$g(M_{\text{cy}}) = 0 \qquad (B.12)$$

with

$$g(x) \equiv 4x^3 - \left(4m \pm \frac{f}{\pi\kappa} + 3M_{\text{sp}}\right)x^2 + \left(4m \pm \frac{f}{\pi\kappa}\right)M_{\text{sp}}x - mM_{\text{sp}}^2 \qquad (B.13)$$

for the mean curvature M_{cy} of the tube, where the plus and minus sign corresponds to out- and in-tubes, respectively, as before. This equation shows that M_{cy} depends only on three parameters: the spontaneous curvature m, which may be positive or negative, the positive mean curvature M_{sp} of the sphere, and the external force f that pulls on the tube ends. [†]

[†] It is straightforward to extend this approach to vesicles, for which the spherical membrane segment and the tubules consist of different intramembrane phases and, thus, have different elastic parameters.

B.5 Seperation of length scales.

The basic assumption underlying the shapes in Fig. 6 is that the tube radius R_{cy} is much smaller than the curvature radius R_{sp} of the large spherical segment which implies that the physically meaningful solutions of $g(M_{cy}) = 0$ with $g(x)$ as in (B.13) must satisfy

$$|M_{cy}| = \frac{1}{2R_{cy}} \gg M_{sp} \qquad (B.14)$$

with $|M_{cy}| = -M_{cy}$ for in-tubes.

For $m = 0$, the condition (B.14) implies that the external force f must be sufficiently large. Indeed, for $m = 0$, the solution of (B.13) behaves as

$$M_{cy} \approx \pm \frac{f}{4\pi\kappa} \quad \text{for} \quad f \gg 3\pi\kappa M_{sp}, \qquad (B.15)$$

which is physically meaningful since $|M_{cy}| \gg M_{sp}$, but as

$$M_{cy} \approx \tfrac{3}{4} M_{sp} \quad \text{for} \quad f \ll 3\pi\kappa M_{sp}, \qquad (B.16)$$

which respresents an unphysical solution with $M_{cy} \simeq M_{sp}$, Therefore, in the small-f regime with $f \lesssim 3\pi\kappa M_{sp}$, tubes with radius $R_{cy} \ll R_{sp}$ are only possible for nonzero spontaneous curvature.

B.6 Radii of stress-free tubules.

Let us now focus on stress-free tubules in the absence of an external force, i.e., for $f = 0$, and let us first consider the limit of a very large sphere, i.e., the limit of vanishing M_{sp}. In this limit, the solution to (B.13) is easily obtained from the first two terms on the right hand side of this equation, which leads to

$$M_{cy} \approx m \quad \text{for small} \quad M_{sp}. \qquad (B.17)$$

Thus, for $f = 0$, out- and in-tubes with positive and negative mean curvature M_{cy} are only possible for positive and negative spontaneous curvature $m > 0$ and $m < 0$, respectively. It is interesting to note that the limit of vanishing M_{sp} corresponds to a large planar membrane, for which the pressure difference ΔP must vanish in mechanical equilibrium. This property is correctly described by the stress balance condition (B.11), which implies $\Delta P = 0$ for $f = 0$ and $M_{cy} = 0$.

A combination of the asymptotic equality (B.17) with the condition (B.14) implies that the spontaneous curvatures must satisfy

$$m \gg M_{sp} \text{ (out-tube)} \quad \text{and} \quad -m \gg M_{sp} \text{ (in-tube)}, \qquad (B.18)$$

i.e., their absolute values must be large compared to $M_{\mathrm{sp}} = 1/R_{\mathrm{sp}}$.

In these regimes, the equation $g(M_{\mathrm{cy}}) = 0$ as given by (B.13) with $f = 0$ has only one solution, [‡] which behaves as

$$M_{\mathrm{cy}} \approx m - \tfrac{1}{4} M_{\mathrm{sp}} \left[1 - \tfrac{1}{4} \left(\frac{M_{\mathrm{sp}}}{m} \right)^2 \right] \quad \text{for small } M_{\mathrm{sp}}/|m| = 2R_{\mathrm{cy}}/R_{\mathrm{sp}} .$$

$$(B.19)$$

The functional form of this solution applies to both out- and in-tubes.

B.7 Tube radii in the presence of external pulling forces.

If the external force f pulls at the end of the tubes, the cubic equation $g(M_{\mathrm{cy}}) = 0$ with $g(x)$ as in (B.13) leads to the tube mean curvature

$$M_{\mathrm{cy}} \approx m - \tfrac{1}{4} M_{\mathrm{sp}} \pm \frac{f}{4\pi\kappa} \quad \text{for small } M_{\mathrm{sp}}/|m| = 2R_{\mathrm{cy}}/R_{\mathrm{sp}} \quad (B.20)$$

up to terms of order $M_{\mathrm{sp}}(M_{\mathrm{sp}}/m)^2$ and $(f/\kappa)(M_{\mathrm{sp}}/m)^2$, where the plus and minus sign corresponds again to out- and in-tubes, respectively.

B.8 Many tubules connected to the same vesicle.

It is straightforward to generalize the results just described to several tubules connected to the same spherical vesicle or spherical membrane cap. If we label the different tubules by the index i, each tubule i with radius $R_{\mathrm{cy},i}$ and length L_i gives a contribution to the shape energy $\mathcal{E}$ that has the same form as the single tube contribution in (B.6). The stress-free state of this vesicle then implies $\partial\mathcal{E}/\partial R_{\mathrm{cy},i} = 0$ and $\partial\mathcal{E}/\partial L_i = 0$. Apart from the index i, all of these equations lead again to the stress balance relations (B.9) and (B.11). This simple structure has two immediate consequences:
(i) A spherical vesicle cannot be connected, at the same time, to both stress-free out-tubes and stress-free in-tubes; and
(ii) When connected to the same vesicle, all stress-free out- and in-tubes have the same radius as given by (57) and (58), respectively, provided all membrane segments have the same composition and, thus, the same elastic properties.

[‡] The uniqueness of the solution can be shown by close inspection of the functional form of $g(x)$. This function has two extrema with $\partial g(x)/\partial x = 0$ at $x_1 = \tfrac{1}{2} M_{\mathrm{sp}}$ and $x_2 = \tfrac{2}{3} m$ where the first extremum has a negative g-value since $g(\tfrac{1}{2} M_{\mathrm{sp}}) = -\tfrac{1}{4} M_{\mathrm{sp}}^3 < 0$.

B.9 Pressure ranges for stable spheres and cylinders.

The stability of membrane tubes has been theoretically studied in Refs.[4–6]. For $f = 0$, i.e., in the absence of external pulling forces, the results of these studies imply that tubes are only stable if the osmotic pressure difference $P_{cy} = P_{cy,in} - P_{cy,ex}$ across the tube membrane is negative and satisfies the inequalities

$$-P^*_{cy} < P_{cy} \leq 0 \quad \text{(stable tubes)} \tag{B.21}$$

with the pressure threshold

$$P^*_{cy} \equiv 3\kappa/R^3_{cy} \tag{B.22}$$

that depends only on the tube radius R_{cy} and the bending rigidity κ but not on the spontaneous curvature m. [§]

The stability criterion for the tube pressure P_{cy} as given by (B.21) must now be compared with the pressure difference ΔP that characterizes stress-free tubes. This pressure difference is given by

$$\Delta P = 16\kappa M^2_{cy}(m - M_{cy}) \approx 4\kappa m^2 M_{sp} - 2\kappa m M^2_{sp} \tag{B.23}$$

as follows from a combination of the expression (B.11) for ΔP with the asymptotic equality $M_{cy} \approx m - \frac{1}{4}M_{sp}$, see (B.19), for the tubes' mean curvature M_{cy}. In addition, since the leading term on the right hand side of (B.23) is positive irrespective of the sign of the spontaneous curvature m, the pressure difference ΔP becomes

$$\Delta P \approx 4\kappa m^2 M_{sp} \approx 4\kappa M^2_{cy} M_{sp} = \kappa/(R^2_{cy} R_{sp}) \quad \text{(stress-free tubes)}, \tag{B.24}$$

a relation that applies to both out- and in-tubes.

A spherical vesicle with radius R_{sp}, on the other hand, is stable if the pressure difference $P_{sp} = P_{sp,in} - P_{sp,ex}$ across its membrane satisfies[4,7]

$$P_{sp} > P^*_{sp} \tag{B.25}$$

with the pressure threshold

$$P^*_{sp} \equiv \frac{4\kappa}{R^3_{sp}}(m R_{sp} - 3) = 4\kappa M^2_{sp}(m - 3M_{sp}) \tag{B.26}$$

that depends on the sphere radius R_{sp}, the bending rigidity κ, and the spontanous curvature m. The pressure thresholds for spherical caps

---

[§] As shown in citebukm96, the pressure threshold P^*_{cy} is also independent of the additional bending rigidity for the area-difference elasticity arising in the absence of flip-flops between the two leaflets of the bilayer membranes.

with curvature radius R_{sp} will, in general, be somewhat different from the expression (B.26) derived for complete spheres with radius R_{sp} but this difference does not affect the results described in the following.

Thus, in order to determine the stability of nanotubes connected to large spheres or spherical caps, we now have to look for a pressure regime, in which tubes are *both stress-free and stable*. In addition, we also need to show that the large spherical segments, to which these tubes are connected, are stable in the same pressure regime.

B.10 Instability of stress-free out-tubes.

Stress-free out-tubes can only occur for sufficiently large *positive* values of the spontaneous curvature m and are characterized by the pressure difference $P_{cy} = P_{cy,in} - P_{cy,ex} = +\Delta P$. In this case, the stability criterion (B.21) leads to

$$-3\kappa/R_c y^3 < \Delta P \leq 0 \qquad (B.27)$$

which contradicts the relation (B.24) for stress-free out-tubes since

$$\Delta P \approx \kappa/(R_{cy}^2 R_{sp}) > 0. \qquad (B.28)$$

Thus, *stress-free out-tubes are unstable* and can only be present as transient structures. This conclusion is in accordance with the results of Ref.[6].

B.11 Stability of stress-free in-tubes.

Stress-free in-tubes can only occur for sufficiently large *negative* values of the spontaneous curvature m and are characterized by the pressure difference $P_{cy} = P_{cy,in} - P_{cy,ex} = -\Delta P$. In this latter case, the stability criterion (B.21) leads to

$$0 \leq \Delta P < 3\kappa/R_{cy}^3 \qquad (B.29)$$

which is consistent with the relation (B.24) for stress-free in-tubes since

$$0 < \Delta P \approx \kappa/(R_{cy}^2 R_{sp}) \ll \kappa/(R_{cy}^3) < 3\kappa/R_c y^3. \qquad (B.30)$$

Thus, *stress-free in-tubes are stable* in contrast to stress-free out-tubes.

This conclusion is confirmed by examining the stability of the large sphere. Now, the pressure threshold P_{sp*} for the sphere as given by (B.26) becomes

$$P_{sp}^* \approx 4\kappa M_{sp}^2 m \approx 4\kappa M_{sp}^2 M_{cy} = -2\kappa/(R_{sp}^2 R_{cy}) \qquad \text{(B.31)}$$

since m and M_{cy} are negative for in-tubes. Thus, the negative spontaneous curvature $m < 0$ enhances the stability of the large sphere and makes the pressure threshold P_{sp}^* negative. Since the sphere is characterized by positive ΔP as in (B.30), one has $\Delta P > P_{sp}^*$ corresponding to a stable sphere. This conclusion should also apply to large spherical caps with curvature radius R_{sp}, even though the eigenmodes will be somewhat different.

References

1 R. Lipowsky, H. G. Döbereiner, C. Hiergeist and V. Indrani, *Physica A*, 1998, **249**, 536–543.
2 R. Lipowsky and H. G. Döbereiner, *Europhys. Lett.*, 1998, **43**, 219–225.
3 R. Lipowsky, M. Brinkmann, R. Dimova, T. Franke, J. Kierfeld and X. Zhang, *J. Phys. Cond. Mat.*, 2005, **17**, S537–S558.
4 Z.-C. Ou-Yang and W. Helfrich, *Phys. Rev. A*, 1989, **39**, 5280–5288.
5 S. Komura and R. Lipowsky, *J. Phys. II France*, 1992, **2**, 1563–1575.
6 D. Bukman, J. Yao and M. Wortis, *Phys. Rev. E*, 1996, **54**, 5463–5468.
7 U. Seifert, K. Berndl and R. Lipowsky, *Phys. Rev. A*, 1991, **44**, 1182–1202.